A Competitive Assay Based on Dual-Mode Au@Pt-DNA Biosensors for On-Site Sensitive Determination of Carbendazim Fungicide in Agricultural Products

Ge Chen[1]*, Rongqi Zhai[1], Guangyang Liu[1], Xiaodong Huang[1], Kaige Zhang[1], Xiaomin Xu[1], Lingyun Li[1], Yanguo Zhang[1], Jing Wang[2], Maojun Jin[2], Donghui Xu[1]* and A. M. Abd El-Aty[3,4,5]

[1] Key Laboratory of Vegetables Quality and Safety Control, Laboratory of Quality and Safety Risk Assessment for Vegetable Products, Ministry of Agriculture and Rural Affairs, Institute of Vegetables and Flowers, Chinese Academy of Agricultural Sciences, Beijing, China, [2] Key Laboratory of Agro-Product Quality and Safety, Ministry of Agriculture and Rural Affairs, Institute of Quality Standard and Testing Technology for Agro-Products, Chinese Academy of Agricultural Sciences, Beijing, China, [3] State Key Laboratory of Biobased Material and Green Papermaking, College of Food Science and Engineering, Qilu University of Technology, Shandong Academy of Science, Jinan, China, [4] Department of Pharmacology, Faculty of Veterinary Medicine, Cairo University, Giza, Egypt, [5] Department of Medical Pharmacology, Faculty of Medicine, Atatürk University, Erzurum, Turkey

Carbendazim (CBZ), a systemic, broad-spectrum benzimidazole fungicide, is widely used to control fungal diseases in agricultural products. Its residues might pose risks to human health and the environment. Therefore, it is warranted to establish a rapid and reliable method for its residual quantification. Herein, we proposed a competitive assay that combined aptamer (DNA) specific recognition and bimetallic nanozyme gold@platinum (Au@Pt) catalysis to trace the CBZ residue. The DNA was labeled onto bimetallic nanozyme Au@Pt surface to produce Au@Pt probes (Au@Pt-DNA). The magnetic Fe_3O_4 was functionalized with a complementary strand of DNA (C-DNA) to form Fe_3O_4 probes (Fe_3O_4-C-DNA). Subsequently, the CBZ and the Fe_3O_4 probes competitively react with Au@Pt probes to form two Au@Pt-DNA biosensors (Au@Pt-ssDNA-CBZ and Au@Pt-dsDNA-Fe_3O_4). The Au@Pt-ssDNA-CBZ biosensor was designed for qualitative analysis through a naked-eye visualization strategy in the presence of CBZ. Meanwhile, Au@Pt-dsDNA-Fe_3O_4 biosensor was developed to quantitatively analyze CBZ using a multifunctional microplate reader. A competitive assay based on the dual-mode Au@Pt-DNA biosensors was established for onsite sensitive determination of CBZ. The limit of detection (LOD) and recoveries of the developed assay were 0.038 ng/mg and 71.88-110.11%, with relative standard deviations (RSDs) ranging between 3.15 and 10.91%. The assay demonstrated a good correlation with data acquired from liquid chromatography coupled with mass spectrometry/mass spectrometry analysis. In summary, the proposed competitive assay based on dual-mode Au@Pt-DNA biosensors might have a great potential for onsite sensitive detection of pesticides in agro-products.

Keywords: carbendazim, Au@Pt-DNA, pesticide residue, biosensor, aptamer

INTRODUCTION

Carbendazim (CBZ) is a broad-spectrum benzimidazole fungicide used to protect a wide variety of crops against fungal disease, thus producing high-quality crops with optimal yields (1, 2). CBZ, which interferes with DNA biosynthesis during fungal cell division, was defined as a major agrochemical pollutant, hazardous to humans and the environment. Because of its long half-life and severe toxicity, residues might threaten safe consumption and negatively influence food quality (3). There is an urgent need to develop analytical methods to determine residual trace levels of CBZ in agro-products to protect public health. To date, a variety of classical quantitive analyses, including liquid chromatography coupled with mass spectrometry (LC-MS) (4) and gas chromatography coupled with tandem mass spectrometry (GC-MS/MS) (5), have been routinely used to monitor CBZ residues in the agricultural products. Although these analytical methods provide high stability and accuracy, preparation steps are laborious, time-consuming, requiring professional operators and expensive instruments (2), restricting their applications. Therefore, a sensitive, rapid, and simple analytical method is needed to detect CBZ. Currently, the rapid immunoassay for detecting CBZ with high sensitivity and specificity (6) overcomes the pitfalls of the traditional analytical methods (7). However, the antibodies are prone to degradation and denaturation during field applications (8), resulting in difficultly in specifically recognizing the target (9). Moreover, antibodies are more complicated, and the manufacturing process is costly and time consuming (10). Furthermore, haptens synthesized from the CBZ analogs can attach to the appropriate functional groups, enabling the conjugation with the protein (11). Hence, a stable, specific, and cost-effective recognition receptor for CBZ is strongly required to replace the traditional immunoassays.

As molecular recognition elements, aptamers are artificially synthesized single-stranded nucleotide sequences, screened through systematic evolution of ligands by exponential enrichment (SELEX) techniques, and could specifically bind the target analyte (12). Aptamers have attracted significant attention because of their advantages of easy synthesis, low cost, and high affinity (13). Unlike antibodies, aptamers are relatively stable under extreme temperature conditions for a short time (14). Therefore, several platforms of aptamer sensors, such as fluorescence (15), colorimetry (16), and electrochemistry (17), have been developed for the detection of pesticides. To improve the stability and sensitivity of aptamer-based assays, nanomaterials (one of the most interesting sensing materials) are bioconjugated with aptamers for selective and sensitive detection of analytes. The nanomaterials with some enzyme-mimicking characteristics are defined as nanozymes (18). Nanozyme, an emerging alternative to the natural enzyme (19), displayed the following advantages: simple preparation methods, high stability, easy surface modification, and low cost (20). Some enzyme-like bimetallic nanomaterials Au@Pt are of great interest because of their multifunctional and synergistic properties (21). Au@Pt combines good chemical stability of Au with specific catalytic activit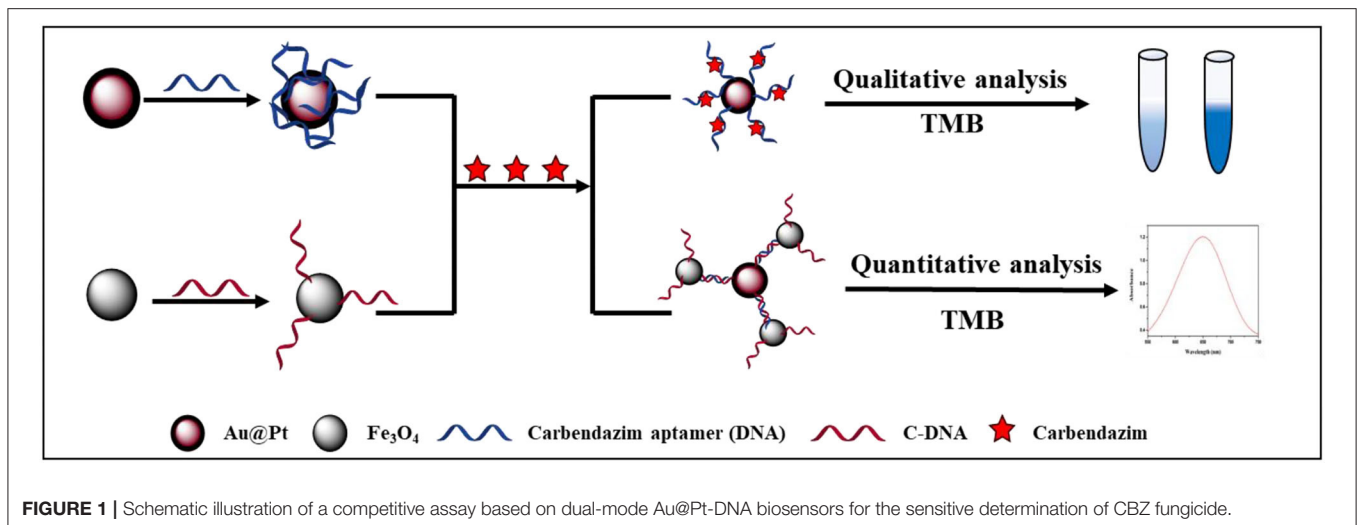ies of Pt (22). Moreover, the DNA could be firmly bound to the surface of Au@Pt (23). Meanwhile, the recent reports have demonstrated that Au@Pt exhibited high-catalytic properties (24, 25).

Herein, a competitive assay based on dual-mode Au@Pt-DNA biosensors for onsite sensitive determination of CBZ fungicide is shown in **Figure 1**. One promising strategy is to reversibly bind target-specific aptamers (DNA) to the Au@Pt surface. The magnetic Fe_3O_4 was functionalized with a complementary strand of DNA (cDNA) to form Fe_3O_4 probes (Fe_3O_4-C-DNA). The CBZ and the Fe_3O_4 probes competitively react with DNA-modified nanozyme Au@Pt to form two Au@Pt-DNA biosensors (Au@Pt-ssDNA-CBZ and Au@Pt-dsDNA-Fe_3O_4 biosensors, respectively). The aptamers only extend from the Au@Pt surface, specifically in the presence of the CBZ (26), which forms Au@Pt-ssDNA-CBZ biosensor for the qualitative analysis through visualization by naked-eye from light blue to dark blue (19). In addition, Au@Pt-dsDNA-Fe_3O_4 biosensor was established for quantitative analysis of CBZ by constructing a calibration curve for trace residual determination of CBZ in agricultural products.

MATERIALS AND METHODS

Materials and Reagents

Gold (Au) chloride hydrate ($HAuCl_4 \bullet xH_2O$), chloroplatinic acid ($H_2PtCl_6 \bullet 6H_2O$), sodium citrate ($C_6H_5Na_3O_7 \bullet 2H_2O$, purity > 99%), Fe_3O_4 (10 mg/ml), 1-ethyl-3-[3-(dimethylamino) propyl] carbodiimide (EDC), and N-hydroxysuccinimide (NHS) were acquired from Sigma-Aldrich (St. Louis, MO, USA). L-ascorbic acid ($C_6H_8O_6$, LAA) was procured from Macklin Biochemical Co., Ltd (Shanghai, China). Carboxyl-functionalized magnetic particles (Fe_3O_4, 10 mg/ml) were secured from Invitrogen (Grand Island, NY). CBZ standard ($C_9H_9N_3O_2$, purity > 99%) was obtained from Dr. Ehrenstorfer GmbH (Augsburg, Germany). Polyethylene glycol 20,000 (PEG 20,000), Tween-20, Tris-EDTA buffer (TE, pH 8.0), and 3,3',5,5'-tetramethylbenzidine (TMB) substrate were purchased from Solarbio (Beijing, China). Primary secondary amine (PSA) and octadecyl (C18) were picked up from Shimadzu (Kyoto, Japan). Anhydrous magnesium sulfate ($MgSO_4$), sodium chloride (NaCl), potassium chloride (KCl), disodium phosphate (Na_2HPO_4), potassium dihydrogen phosphate (KH_2PO_4), and other analytical grade reagents were supplied by Sinopharm Chemical Reagent Co., Ltd. (Beijing, China). Hydrochloric acid (HCl) and nitric acid (HNO_3) were provided by Beijing Chemical Industry Group Co., Ltd. (Beijing, China). The CBZ aptamer (DNA) and C-DNA (the sequence of DNA and C-DNA designed in **Supplementary Table 1**) were synthesized by Sangon Co., Ltd. (Shanghai, China). A 96-well micro-plate (Transplant, flat bottom) was supplied by Costar, Inc. (Kennebunk, ME, USA). The HPLC-grade acetonitrile (ACN) and methanol (MeOH) were obtained from Thermo Fisher Scientific (Pittsburgh, PA, USA). Ultrapure water was purified by a Milli-QRC purification system (Millipore, Bedford, MA, USA). Aqua regia is a mixture of HCl and HNO_3 ($HCl/HNO_3 = 3/1$). The 0.01 M phosphate-buffered saline (PBS buffer, pH 7.4) consists of 0.2 g KCl, 0.27 g KH_2PO_4, 8 g NaCl, and 1.14 g Na_2HPO_4. Washing buffer (PBST:

FIGURE 1 | Schematic illustration of a competitive assay based on dual-mode Au@Pt-DNA biosensors for the sensitive determination of CBZ fungicide.

PBS buffer containing 0.05% Tween-20) was prepared for washing micro-plates.

Preparation of Au@Pt Nanomaterials

The Au@Pt nanomaterials were prepared by the seed-mediated growth method (27). All the glassware was thoroughly soaked in aqua regia and rinsed with ultrapure water. At first, the seeds of gold nanoparticles (AuNPs) were prepared with mirror modifications (28). AuNPs were synthesized by a chemical reduction method where $HAuCl_4$ was used as a precursor, and trisodium citrate was used as a reducing agent and stabilizing agent (29, 30). One milliliter $HAuCl_4$ (10%, *w/v*) aqueous solution and 99 ml distilled water were added to a round-bottomed flask. After that, 10 ml of trisodium citrate (38.8 mM) solution was quickly added when the aforementioned mixture heated to boiling under vigorous stirring and refluxing using a magnetic stirring heater (Zhengzhou, China). The color of the solution was changed from yellow to wine red, and the mixture was left to stir for another 20 min.

Second, Au@Pt was synthesized using AuNPs (30 ml) as seeds as follows: H_2PtCl_6 (1.0 mM, 10 ml) solution and LAA (5 mM, 10 ml) were added to the AuNPs solution and heated to boiling until the color changes from wind red to brown-red. Then, the aforementioned aqueous solution was left to stir for another 30 min to ensure a comprehensive reduction of H_2PtCl_6. The synthetic Au@Pt was cooled to room temperature, stored in the dark at 4°C, and then filtered through a cellulose nitrate filter.

Construction of Au@Pt Probe

Sangon Biotech Co., Ltd. synthesized the aptamer (DNA) of CBZ. The aptamer (DNA) sequence of CBZ was acquired from literature (31). Before using the aptamer (DNA) of CBZ (35.08 μg), it should be activated. At first, 18 μl TE buffer was added into the microcentrifuge tube with the aptamer (DNA) of CBZ to dissolve, and 18 μl TCEP solution was then added to reduce the disulphide bonds to single sulfhydryl groups. Subsequently, the DNA solution was shaken for 3 h under 200 rpm. After that, the activated DNA reacts with Au@Pt solution to form an
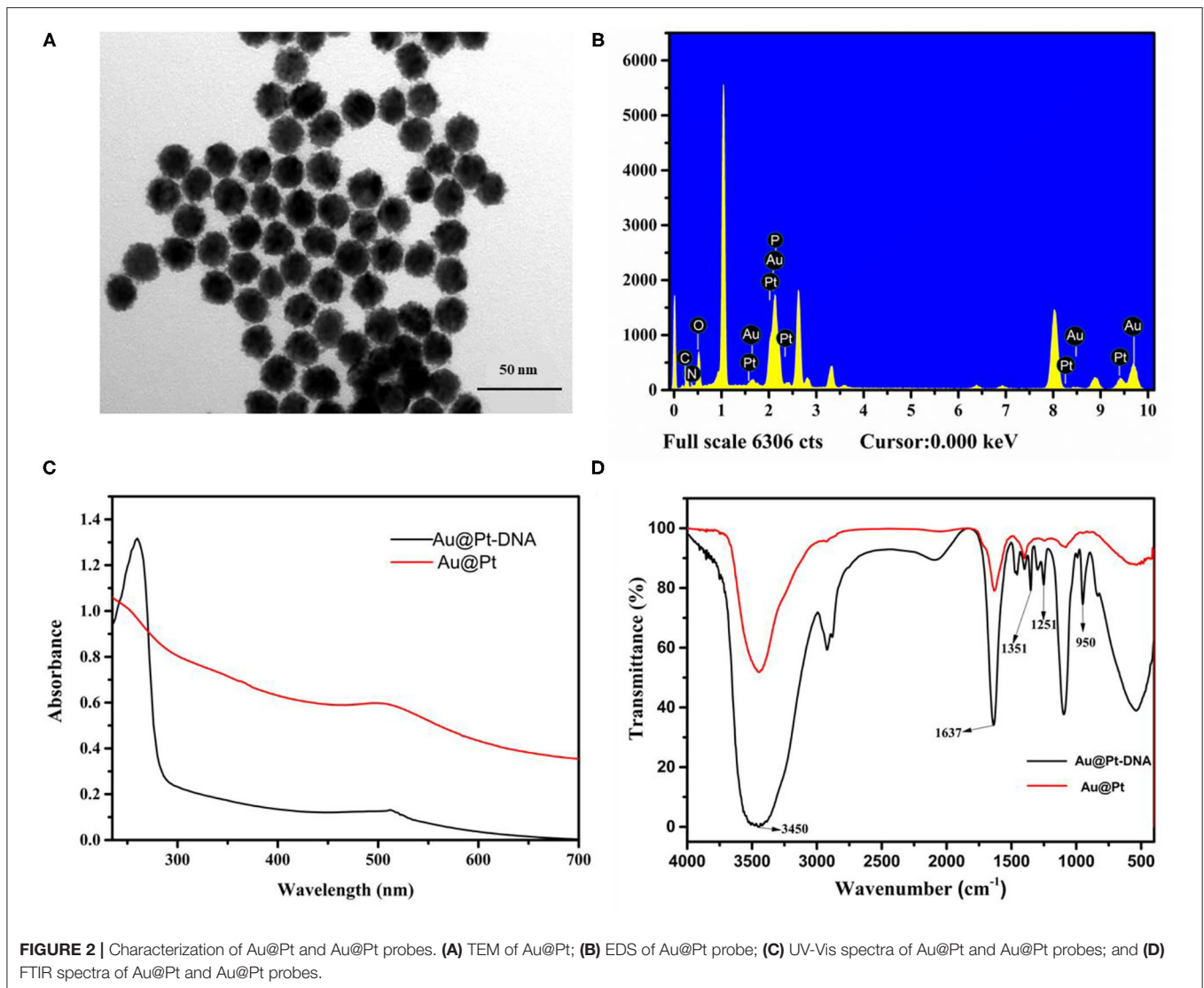
Au@Pt probe (Au@Pt-DNA). The 30% PEG and 0.1 M PBS were selected to stabilize the Au@Pt probe to achieve 0.5% PEG and 0.01 M PBS in the final solution and avoid the aggregation of the Au@Pt probe (Au@Pt-DNA). Afterward, unbound aptamer of CBZ (DNA) was removed by centrifugation at 10,000 rpm for 30 min. The Au@Pt probe was kept refrigerated at 4°C for further analysis.

Construction of Fe_3O_4 Probe

At first, the C-DNA (33.26 μg) should be activated before conjugation with Fe_3O_4. The TE buffer (pH 8.5, 18 μl) was added to the C-DNA. Next, the NHS (10 mg/ml, 100 μl) and EDC (10 mg/ml, 100 μl) were selected to activate the carboxyl group of Fe_3O_4 (10 μl, 10 mg/ml) with gentle shaking for 30 min. The Fe_3O_4 was magnetically separated and washed three times with MES buffer (15 mM) for 1 min. The washed Fe_3O_4 was resuspended in PBS buffer (pH 7.4, 0.1 mol/L). After that, the activated C-DNA was added to Fe_3O_4 solution to construct Fe_3O_4 probe (Fe_3O_4-C-DNA) for 18 h at 4°C. The Fe_3O_4 probe was washed three times with PBS buffer to remove the unconjugated C-DNA. Finally, the Fe_3O_4 probe was resuspended in 500 μl PBS (pH 7.4, 0.1 mol/L) and stored at 4°C for further use.

A Competitive Assay Based on Au@Pt-DsDNA-Fe_3O_4 Biosensor

In general, the quantitative analysis of CBZ was carried out as follows: at first, 150 μl Au@Pt-DNA (0.3 nmol/L) was added to a 0.5-ml microcentrifuge tube. Then, different concentrations of CBZ standard were prepared by PBS solution containing 10% methanol or supernatant of actual samples extract in advance. Afterward, 60 μl CBZ was added to Au@Pt-DNA solution, followed by adding a 60 μl Fe_3O_4 probe (diluted by probe buffer, 0.1 mg/L) to construct a competitive assay at room temperature. The aforementioned mixture was washed three times, followed by separation under a magnetic field for 1 min. After that, the Au@Pt-dsDNA-Fe_3O_4 mixture was resuspended

FIGURE 2 | Characterization of Au@Pt and Au@Pt probes. **(A)** TEM of Au@Pt; **(B)** EDS of Au@Pt probe; **(C)** UV-Vis spectra of Au@Pt and Au@Pt probes; and **(D)** FTIR spectra of Au@Pt and Au@Pt probes.

in PBS buffer to catalyze TMB for the trace detection of CBZ using a multifunctional microplate reader (Salzburg, Austria).
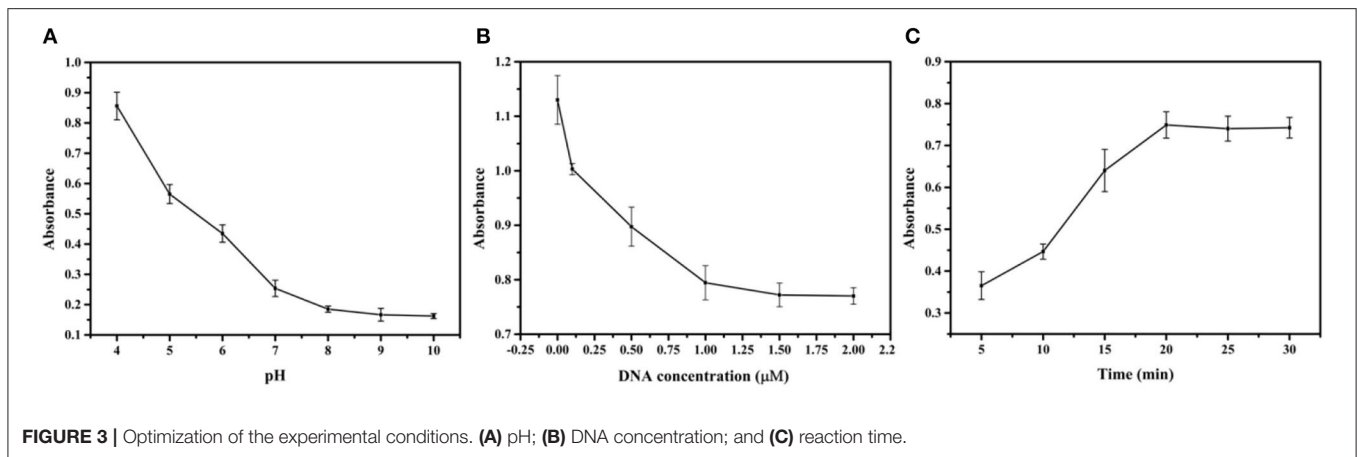
Sample Preparation

The leeks and rice samples were obtained from the Shangdong vegetable production field to evaluate the feasibility of the developed assay. Blank samples (free from CBZ) were used for creating a calibration curve and recovery experiments. The leeks and rice samples were pretreated with QuEChERS (quick, easy, cheap, effective, rugged, and safe) method designed by the Anastassiades team (32) with slight modifications. Standard concentrations (10, 50, and 100 $\mu g \cdot kg^{-1}$) were used as spiking levels to homogenized samples (10 g for leeks, 5 g for rice) in 50-ml centrifuge tubes. Afterward, the spiked samples were allowed to equilibrate at room temperature for 4 h. Subsequently, 10 ml acetonitrile was added, followed by a 2 min vortex mix. Next, 2 g anhydrous $MgSO_4$ and 1 g NaCl were added for dehydration and stratification (vigorous shaking for 1 min). The supernatant was

transferred into a 10-ml plastic tube, vortexed for another 1 min, and centrifuged at 5,000 rpm (at 4°C) for 5 min. Subsequently, 5 ml supernatant was purified using a purification cartridge (52 mg PSA, 52 mg C18, and 26 mg GCB), vortexed again for 1 min, and then centrifuged at 10,000 rpm (at 4°C) for 5 min. Finally, the supernatant was filtered through a 0.22-μm filter (Jinteng, China) for competitive assay based on Au@Pt-dsDNA-Fe_3O_4 biosensor and LC-MS/MS analysis.

RESULTS

Characterization of Au@Pt and Au@Pt Probe

Using Au as seeds, a thin Pt layer was deposited on the surface of the Au core to achieve Au@Pt. The morphology of Au@Pt nanoparticles was characterized by transmission electron microscopy (TEM). As shown in **Figure 2A**, the Au@Pt showed uniform spherical shapes with an average

FIGURE 3 | Optimization of the experimental conditions. **(A)** pH; **(B)** DNA concentration; and **(C)** reaction time.

particle size of 20 nm. Compared with smooth Au (as shown in **Supplementary Figure 1A**). The particle size of Au@Pt was increased by ∼5 nm indicating the existence of smooth AuNPs surface of a 5 nm layer Pt. The TEM images of Au@Pt demonstrated that the Au@Pt core-shell structure was successfully prepared. Then, the Au@Pt and Au@Pt probes were carefully characterized by energy dispersive spectrometer (EDS). As presented in **Figure 2B**, the EDS of Au@Pt probe has shown that P element signal except for Au and Pt, which are from Au@Pt nanoparticles (as depicted in **Supplementary Figure 1B**). Therefore, the P characteristic element can be inferred from the DNA. The EDS (Hitachi Co., Ltd., Tokyo, Japan) of Au@Pt and Au@Pt probes indicate that the DNA was successfully modified on the Au@Pt surface. To further confirm the successful preparation of the Au@Pt probe, the UV–vis spectra (Shimadzu, Japan) were used to verify the synthesized Au@Pt probe. The UV–vis spectra of Au@Pt (red line) have a maximum absorbance at 508 nm. Compared with Au@Pt, a prominent characteristic absorbance peak near 260 nm was noticed in UV–vis spectroscopy of Au@Pt probe (black line), as presented in **Figure 2C**. As reported, the maximum absorption peak of DNA occurs at 260 nm (23), denoting that the Au@Pt surface was conjugated with DNA. In addition, the Au@Pt probe was characterized by FT-IR (Pittsburgh, USA), as depicted in **Figure 2D**. Peaks around 3,450 and 1,637 cm^{-1} are derived from the O–H stretching, representing the H-O-H bending vibration of water. The characteristic peaks of 1,351, 1,251, and 950 cm^{-1} were observed except for 3,450 and 1,637 cm^{-1} in the Fourier-transform infrared spectroscopy (FTIR) spectra of the Au@Pt probe. These characteristic peaks, corresponding to C=C, C-N, and C-H, respectively, can be inferred from bases of DNA. These results denote that the DNA was successfully modified on the surface of Au@Pt.
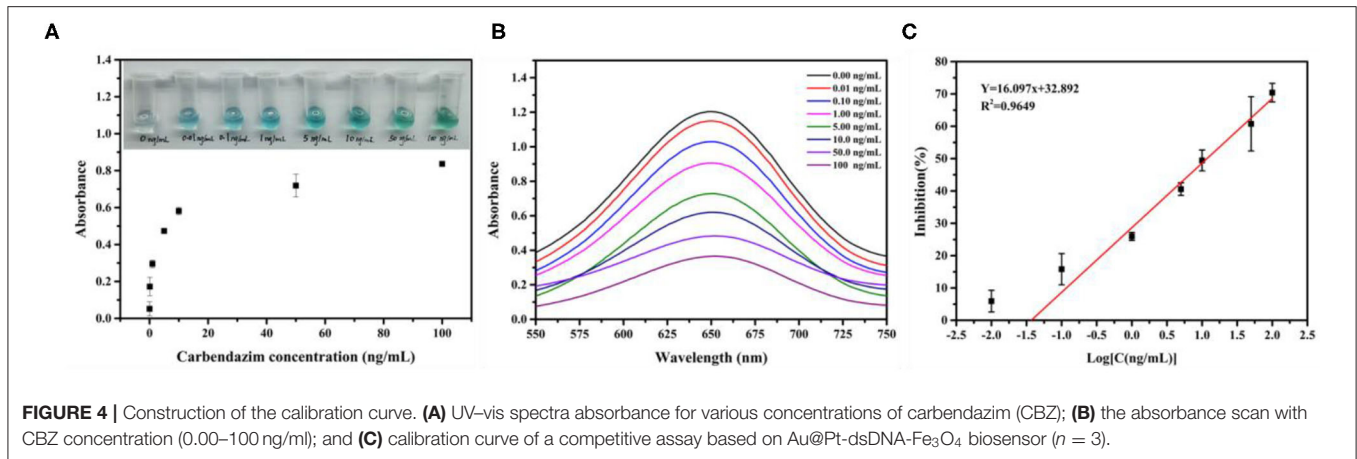
Optimization of the Experimental Conditions

This section investigated the influence of important factors, such as pH value, DNA concentration, and reaction time, to achieve the optimal experimental conditions for CBZ detection. The pH plays a crucial role in the preparation of the Au@Pt probe. A

series of pH ranges (4.0, 5.0, 6.0, 7.0, 8.0, 9.0, and 10.0) was set to estimate the optimal value for forming the Au@Pt probe. The catalytic efficiency of the Au@Pt probe was decreased with increasing the pH value to 8.0 (as depicted in **Figure 3A**). The DNA is easily degraded under acidic conditions (low pH value). The Au@Pt probe catalytic efficiency was increased because more catalytic active sites were exposed with a low concentration of DNA modified on the surface of Au@Pt nanomaterials. Thus, the optimal pH value was set at 8.0 for this assay. The sensitivity of the competitive assay based on Au@Pt-dsDNA-Fe_3O_4 biosensor depends on the DNA concentrations modified on the surface of Au@Pt. Then, the DNA concentration was carefully optimized as well. Different DNA concentrations (0, 0.1, 0.5, 1.0, 1.5, and 2.0 µM) were designed to prepare the Au@Pt probe. Like the influence of pH, the catalytic efficiency of the Au@Pt probe was reduced with a high concentration of DNA, as can be displayed from **Figure 3B**, reaching maximum absorbance at 1.0 µM. Notably, this evidence demonstrated that the optimal concentration of DNA was 1.0 µM in this assay. It is essential to optimize the reaction time between CBZ and Au@Pt probe to detect CBZ rapidly. In turn, a set of reaction times (5, 10, 15, 20, 25, and 30 min) were designed to achieve the optimal reaction time. As time increased, the catalytic efficiency of the Au@Pt probe was improved, reaching the maximum absorbance at 20 min (as shown in **Figure 3C**). Thus, 20 min was identified as the optimized reaction time for the following experiments.

Qualitative Analysis

The CBZ and the Fe_3O_4 probe competitively react with DNA-modified nanomaterials Au@Pt to form Au@Pt-ssDNA-CBZ biosensor and Au@Pt-dsDNA-Fe_3O_4 biosensor, respectively. The Au@Pt-ssDNA-CBZ biosensor solution color dramatically changed from light blue to dark blue with Au@Pt-ssDNA-CBZ biosensor to catalyze TMB when the concentration of CBZ increased from 0 to 100 ng/ml (as shown in **Figure 4A**). The catalytic efficiency of the Au@Pt-ssDNA-CBZ biosensor was improved by increasing the CBZ concentration. The Au@Pt-ssDNA-CBZ biosensor catalytic efficiency was increased because more catalytic active sites were exposed in the presence of CBZ, which was bonded to the DNA on the surface of

FIGURE 4 | Construction of the calibration curve. **(A)** UV–vis spectra absorbance for various concentrations of carbendazim (CBZ); **(B)** the absorbance scan with CBZ concentration (0.00–100 ng/ml); and **(C)** calibration curve of a competitive assay based on Au@Pt-dsDNA-Fe$_3$O$_4$ biosensor ($n = 3$).

TABLE 1 | Calibration curve of carbendazim (CBZ) in field incurred samples ($n = 3$).

Samples	Spiked concentration (ng/mg)	Recovery (%)	RSD (%)	IC$_{50}$ (ng/mg)	LOD (ng/mg)	R^2
Leek	10	71.88 ± 0.04	10.91	7.56	0.044	0.9613
	50	96.40 ± 0.01	3.93			
	100	110.11 ± 0.02	6.76			
Rice	10	91.62 ± 0.03	6.52	6.08	0.041	0.9453
	50	89.86 ± 0.01	4.21			
	100	107.45 ± 0.01	3.16			

C_{50}: Represents the concentration at which a substance exerts half of its maximal inhibitory effect.

Au@Pt nanomaterials. Hence, the designed Au@Pt-ssDNA-CBZ biosensor could use as a qualitative analysis biosensor for on-site pesticide monitoring in the agro-products.

Quantitative Analysis (Calibration Curves)

The calibration curve was established based on Au@Pt-dsDNA-Fe$_3$O$_4$ biosensor catalysis in the competitive assay. The absorbance intensity decreased as the CBZ concentration increased in this study, as depicted in **Figure 4B**. It displayed a maximum absorbance at 650 nm. The calibration curve of the competitive assay based on Au@Pt-dsDNA-Fe$_3$O$_4$ biosensor for detection of CBZ pesticide was established under the optimal condition (**Figure 4C**). The calibration regression equation of curve ($Y = 16.097x + 32.892$) was achieved with a wide linear range. Y represented the inhibition rate (%) and the logarithmic (Log) concentration of CBZ as the X abscissa axis. A low-detection limit (0.038 ng/mg) was acquired with a good linear relationship ($R^2 = 0.9649$). The RSDs ranged from 1.56 to 10.22%. The LOD of this assay was lower than the maximum residue limit (MRL) of CBZ enacted by China (GB 2763–2021) in various agro-products.

Assay Evaluation

The method was validated in terms of accuracy, precision, and LODs. The accuracy (recoveries of the proposed assay),

precision (RSDs of the proposed assay), LODs, and correlation coefficients (R^2 of regression equation) were used to evaluate the reliability, applicability, and sensitivity of the assay. To determine the validation parameters, three concentrations (10, 50, and 100 ng/mg) of CBZ standard solutions were chosen. For leek samples, the average recoveries ranged from 71.88 to 110.11% with RSDs (3.93–10.91%), and a low LOD (0.044 ng/mg) and IC$_{50}$ (7.56 ng/mg) were acquired in the competitive assay. Like leeks', average recoveries of rice, RSDs, LOD, and IC$_{50}$ were 89.86–107.45%, 4.21–6.52%, 0.041 ng/mg and 6.08 ng/mg, respectively (**Table 1**). The regression equations were $Y = 17.905x + 34.267$ and $Y = 18.718x + 36.535$ for leeks and rice, respectively. Hence, good correlations (R^2 0.9613 for leeks and 0.9453 for rice) were gained using the competitive assay (**Table 1**, **Supplementary Figure 3**). Therefore, the Au@Pt-dsDNA-Fe$_3$O$_4$ biosensor of this competitive assay holds the potential as a sensitive and reliable assay for residual trace detection of pesticides.

Specificity

Specificity, recognizing the target molecule, is essential in the performance evaluation [33]. The accuracy of the assay method is mainly based on the specificity of the CBZ aptamer [2]. Several commonly used fungicides and insecticides (100 ng/ml solution of imidacloprid, procymidone, chlorpyrifos, and acetamiprid)
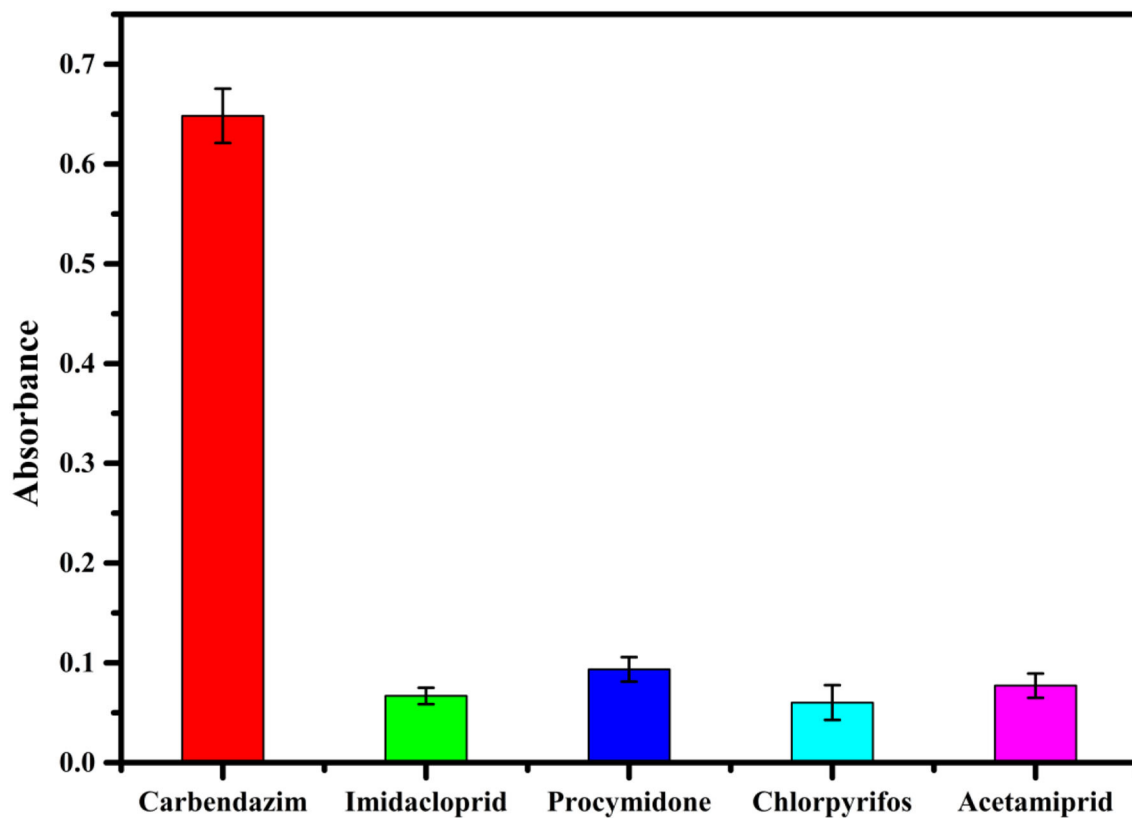
FIGURE 5 | Specificity between CBZ and other unrelated pesticides.

were investigated to evaluate the specificity of the proposed competitive assay for detection of CBZ. As can be inferred from **Figure 5**, the absorbance of the Au@Pt-ssDNA-CBZ biosensor increased only in the presence of CBZ. In contrast, other pesticides caused minor changes in absorbance. Hence, imidacloprid, procymidone, chlorpyrifos, and acetamiprid have a negligible effect on the proposed competitive assay in the presence of CBZ.

Confirmation Analysis

To further confirm the proposed accuracy of the assay, the blank leeks and rice samples were randomly selected to establish the correlation between the competitive assay and LC-MS/MS method (the parameters of LC-MS/MS shown in **Supplementary Table 2**). Five concentrations (5, 10, 20, 50, and 100 ng/mg) of CBZ were spiked to blank leek ($n = 24$) and rice ($n = 24$) samples with vigorous shaking. Half of the samples were analyzed by the proposed competitive assay based on Au@Pt-dsDNA-Fe$_3$O$_4$ biosensor, and the rest were quantified with LC-MS/MS. The correlation coefficients were achieved to assess the association between both methods. The correlation coefficients were 0.9339 and 0.9321 for leek and rice, respectively (**Figure 6**, **Supplementary Table 3**). These findings denote that competitive assay has good reliability to satisfy the requirements for pesticide detection in agro-products.

DISCUSSION

This study proposed dual-mode Au@Pt-DNA biosensors (Au@Pt-ssDNA-CBZ biosensor and Au@Pt-dsDNA-Fe^{3}O^4 biosensor) to analyze CBZ residues agricultural products.

The construction of the Au@Pt probe is the main key factor for Au@Pt-DNA biosensors. The EDS, UV–vis and FT-IR techniques were used to characterize the Au@Pt probe. Compared with Au@Pt nanoparticles (as depicted in **Supplementary Figure 1B**), the EDS of the Au@Pt probe has shown a P element signal (**Figure 2B**). It has been deduced that the P element is derived from DNA. A prominent characteristic absorbance peak (near 260 nm) was noticed in UV–vis spectroscopy of the Au@Pt probe (**Figure 2C**). As reported, the maximum absorption peak of DNA occurs at 260 nm [23]. The characteristic peaks of 1,351, 1,251, and 950 cm^{-1}, corresponding to C=C, C-N, and C-H, were observed in the FTIR spectra of the Au@Pt probe, as shown in **Figure 2D**. These results denote that the Au@Pt probe was successfully prepared.

The pH value, DNA concentration, and reaction time were investigated for establishing the assay based on Au@Pt-DNA biosensors to detect CBZ. The DNA is easily degraded under acidic conditions. The catalytic efficiency of the Au@Pt probe achieved the best results when the pH value reached 8.0 (**Figure 3A**). Similarly, the concentration of DNA at 1.0 μM, the catalytic efficiency of the Au@Pt probe reached maximum
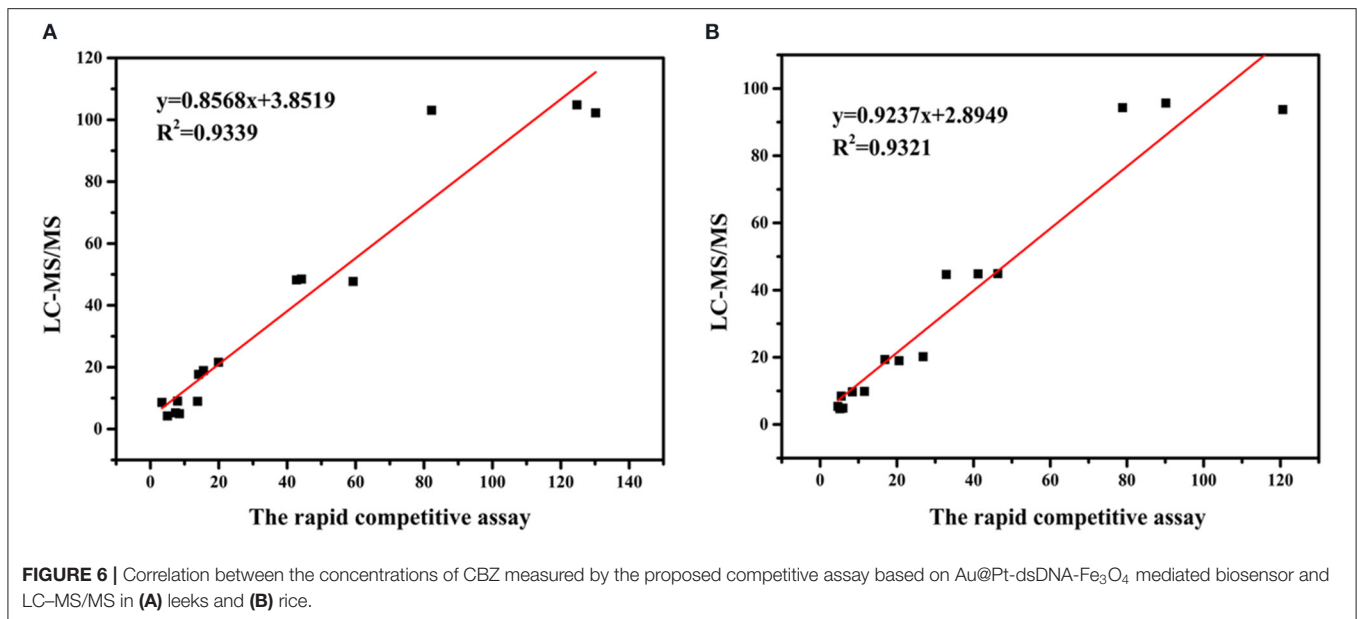
FIGURE 6 | Correlation between the concentrations of CBZ measured by the proposed competitive assay based on Au@Pt-dsDNA-Fe$_3$O$_4$ mediated biosensor and LC–MS/MS in **(A)** leeks and **(B)** rice.

absorbance (**Figure 3B**). The Au@Pt probe with low DNA concentration achieves poor sensitivity. However, the higher DNA concentration inhibits the Au@Pt probe catalysis efficiency because too much DNA concentration might be covering the catalytic site on the Au@Pt nanozyme.

The Au@Pt-ssDNA-CBZ biosensor solution color dramatically changed from light blue to dark blue with Au@Pt-ssDNA-CBZ biosensor to catalyze TMB when the concentration of CBZ increased from 0 to 100 ng/ml (as shown in **Figure 4A**). The catalytic efficiency of the Au@Pt-ssDNA-CBZ biosensor improved by increasing the CBZ concentration because more catalytic active sites of Au@Pt were exposed in the presence of CBZ that was bonded to the DNA on the surface of Au@Pt nanomaterials. Hence, the designed Au@Pt-ssDNA-CBZ biosensor could use as a qualitative analysis biosensor for on-site pesticide monitoring in agro-products through naked-eye visualization.

In addition, the Au@Pt-dsDNA-Fe$_3$O$_4$ biosensor was regarded as quantitate analysis biosensor to establish a sensitive and reliable assay for residual trace detection of pesticides. The regression equation of calibration curve' ($Y = 16.097x + 32.892$, $R^2 = 0.9649$) was achieved. This assay acquired a low LOD (0.038 ng/mg) with RSDs ranged from 1.56 to 10.22% (**Figure 4C**). The leeks and rice samples were selected to monitor the residual levels of CBZ using the proposed assay. As shown in **Table 1**, the mean recoveries (leeks: 71.88–110.11%, rice: 89.86–107.45%) meet the EU guidance document for pesticide residue testing (SANTE/11813/2017). This assay acquired a low LOD (0.038 ng/mg) with RSDs ranging from 1.56 to 10.22%. Therefore, the Au@Pt-dsDNA-Fe$_3$O$_4$ biosensor of this competitive assay holds the potential as a sensitive and reliable assay for residual trace detection of pesticides. Compared with other assays based on nanomaterials, such as Au/Fe$_3$O$_4$ (6), UCNPs-MnO$_2$ (34), AuNPs (35, 36), Nd$_2$O$_3$ (37), and MoS$_2$/MWCNTs (38) for CBZ detection is compiled in **Table 2**. As shown, this proposed

TABLE 2 | Various assays for detection of CBZ based on nanomaterials.

Nanomaterials	Recovery (%)	LOD	Reference
Au@Pt	71.88–110.11%	0.037 ng/mg	This work
Au/Fe$_3$O$_4$	102.4–115.0%	0.44 ng/ml	(6)
UCNPs-MnO$_2$	85.58–109.40%	0.05 ng/ml	(34)
AuNPs	94.9–104.8%	2.2 nM	(35)
AuNPs	96.3–111.2%	2.33 nM	(36)
Nd$_2$O$_3$	-	0.027 mM	(37)
MoS$_2$/MWCNTs	89.18–105.56%	7.4 nM	(38)

competitive assay based on dual-mode Au@Pt-DNA biosensors acquires much lower LOD than other nanomaterials. Besides, the LOD of this assay is much lower than the MRL of CBZ set by China in various agro-products.

CONCLUSIONS AND FUTURE PERSPECTIVES

A competitive assay based on dual-mode Au@Pt-DNA biosensors combined aptamer (DNA) specific recognition property, bimetallic nanomaterials Au@Pt catalysis, and Fe$_3$O$_4$ magnetic separation was proposed to trace the CBZ residue. The qualitative Au@Pt-ssDNA-CBZ biosensor with aptamer (DNA) specific recognition property monitors pesticides through light blue to dark blue visualization and quantitative Au@Pt-dsDNA-Fe$_3$O$_4$ biosensor with bimetallic nanomaterials Au@Pt catalysis and Fe$_3$O$_4$ magnetic separation detect CBZ residue, respectively. Overall, this proposed competitive assay holds the potential as a sensitive and reliable assay for residual trace detection of pesticides and can be used for rapid on-site pesticide

monitoring, reducing false-negative results, and improving screening efficiency and sensitivity.

DATA AVAILABILITY STATEMENT

The original contributions presented in the study are included in the article/**Supplementary Material**, further inquiries can be directed to the corresponding authors.

AUTHOR CONTRIBUTIONS

GC and DX investigated, designed, and wrote the original draft. RZ, GL, and XH investigated and supervised the article. KZ, XX, LL, and YZ visualized and investigated. MJ, JW, and AA were involved in investigation and writing (review and editing) the manuscript. All the authors contributed to the article and approved the submitted version.

SUPPLEMENTARY MATERIAL

The Supplementary Material for this article can be found online at: https://www.frontiersin.org/articles/10.3389/fnut.2022.820150/full#supplementary-material

REFERENCES

1. Chuang S, Yang H, Wang X, Xue C, Jiang J, Hong Q. Potential effects of Rhodococcus qingshengii strain djl-6 on the bioremediation of carbendazim-contaminated soil and the assembly of its microbiome. *J Hazard Mater.* (2021) 414:125496. doi: 10.1016/j.jhazmat.2021.125496

2. Fu R, Zhou J, Liu Y, Wang Y, Liu H, Pang J, et al. Portable and quantitative detection of carbendazim based on the readout of a thermometer. *Food Chem.* (2021) 351:129292. doi: 10.1016/j.foodchem.2021.129292

3. Liu Z, Chen Y, Han J, Chen D, Yang G, Lan T, et al. Determination, dissipation dynamics, terminal residues and dietary risk assessment of thiophanate-methyl and its metabolite carbendazim in cowpeas collected from different locations in China under field conditions. *J Sci Food Agric.* (2021) 101:5498–507. doi: 10.1002/jsfa.11198

4. Li P, Sun P, Dong X, Li B. Residue analysis and kinetics modeling of thiophanate-methyl, carbendazim, tebuconazole, and pyraclostrobin in apple tree bark using QuEChERS/HPLC-VWD. *Biomed Chromatogr.* (2020) 34:e4851. doi: 10.1002/bmc.4851

5. Chu Y, Tong Z, Dong X, Sun M, Gao T, Duan J, et al. Simultaneous determination of 98 pesticide residues in strawberries using UPLC-MS/MS and GC-MS/MS. *Microchem J.* (2020) 156:104975. doi: 10.1016/j.microc.2020.104975

6. Li Q, Dou X, Zhao X, Zhang L, Luo J. Xing, X, et al. A gold/Fe₃O₄ nanocomposite for use in a surface plasmon resonance immunosensor for carbendazim. *Microchim Acta.* (2019) 186:313. doi: 10.1007/s00604-019-3402-0

7. Koukouvinos G, Karachaliou CE, Raptis I, Petrou P, Livaniou E, Kakabakos S. Fast and sensitive determination of the fungicide carbendazim in fruit juices with an immunosensor based on white light reflectance spectroscopy. *Biosensors.* (2021) 11:153. doi: 10.3390/bios11050153

8. Qiao Q, Guo X, Wen F, Chen L, Xu Q, Zheng N, et al. Aptamer-based fluorescence quenching approach for detection of aflatoxin M1 in milk. *Front Chem.* (2021) 9:653869. doi: 10.3389/fchem.2021.653869

9. Zhao X, Zhang X, Qin M, Song Y, Zhang J, Xia X, et al. Determination of carbendazim by aptamer-based fluorescence resonance energy transfer (FRET). *Anal Lett.* (2020) 54:2198–210. doi: 10.1080/00032719.2020.1849250

10. Zikos C, Evangelou A, Karachaliou CE, Gourma G, Blouchos P, Moschopoulou G, et al. Commercially available chemicals as immunizing haptens for the development of a polyclonal antibody recognizing carbendazim and other benzimidazole-type fungicides. *Chemosphere.* (2015) 119:16–20. doi: 10.1016/j.chemosphere.2014.03.049

11. Yan H, Liu L, Xu N, Kuang H, Xu C. Development of an immunoassay for carbendazim based on a class-selective monoclonal antibody. *Food Agric Immunol.* (2015) 26:659–70. doi: 10.1080/09540105.2015.1007446

12. Zhou W, Huang PJ, Ding J, Liu J. Aptamer-based biosensors for biomedical diagnostics. *Analyst.* (2014) 139:2627–40. doi: 10.1039/c4an00132j

13. Fan K, Yang R, Zhao Y, Zang C, Miao X, Qu B, et al. A fluorescent aptasensor for sensitive detection of isocarbophos based on AT-rich three-way junctions DNA templated copper nanoparticles and Fe₃O₄@GO. *Sens Actuators B.* (2020) 321:128515. doi: 10.1016/j.snb.2020.128515

14. McConnell EM, Nguyen J, Li Y. Aptamer-based biosensors for environmental monitoring. *Front Chem.* (2020) 8:434. doi: 10.3389/fchem.2020.00434

15. Shi YQ Li WT, Feng XP, Lin L, Nie PC, Shi JY, et al. Sensing of mercury ions in Porphyra by Copper@Gold nanoclusters based ratiometric fluorescent aptasensor. *Food Chem.* (2021) 344:10. doi: 10.1016/j.foodchem.2020.128694

16. Zhang WW, Wang YL, Nan MN Li YC, Yun JM, Wang Y, et al. Novel colorimetric aptasensor based on unmodified gold nanoparticle and ssDNA for rapid and sensitive detection of T-2 toxin. *Food Chem.* (2021) 348:8. doi: 10.1016/j.foodchem.2021.129128

17. Nan MN Bi Y, Xue HL, Long HT, Xue SL, Pu LM, et al. Modification performance and electrochemical characteristics of different groups of modified aptamers applied for label-free electrochemical impedimetric sensors. *Food Chem.* (2021) 337:6. doi: 10.1016/j.foodchem.2020.127761

18. Wei H, Wang EK. Nanomaterials with enzyme-like characteristics (nanozymes): next-generation artificial enzymes. *Chem Soc Rev.* (2013) 42:6060–93. doi: 10.1039/c3cs35486e

19. Weerathunge P, Behera BK, Zihara S, Singh M, Prasad SN, Hashmi S, et al. Dynamic interactions between peroxidase-mimic silver nanozymes and chlorpyrifos-specific aptamers enable highly-specific pesticide sensing in river water. *Anal Chim Acta.* (2019) 1083:157–65. doi: 10.1016/j.aca.2019.07.066

20. Wang Q, Wei H, Zhang Z, Wang E, Dong S. Nanozyme: An emerging alternative to natural enzyme for biosensing and immunoassay. *TrAC, Trends Anal Chem.* (2018) 105:218–24. doi: 10.1016/j.trac.2018.05.012

21. Sim S, Beierle A, Mantos P, McCrory S, Prasankumar RP, Chowdhury S. Ultrafast relaxation dynamics in bimetallic plasmonic catalysts. *Nanoscale.* (2020) 12:10284–91. doi: 10.1039/D0NR00831A

22. Lu C, Tang L, Gao F, Li Y, Liu J, Zheng J. DNA-encoded bimetallic Au-Pt dumbbell nanozyme for high-performance detection and eradication of *Escherichia coli* O157:H7. *Biosens Bioelectron.* (2021) 187:113327. doi: 10.1016/j.bios.2021.113327

23. Chen G, Liu G, Jia H, Cui X, Wang Y, Li D, et al. A sensitive bio-barcode immunoassay based on bimetallic Au@Pt nanozyme for detection of organophosphate pesticides in various agro-products. *Food Chem.* (2021) 362:130118. doi: 10.1016/j.foodchem.2021.130118

24. Tian J, Liang Z, Hu O, He Q, Sun D, Chen Z. An electrochemical dual-aptamer biosensor based on metal-organic frameworks MIL-53 decorated with Au@Pt nanoparticles and enzymes for detection of COVID-19 nucleocapsid protein. *Electrochim Acta.* (2021) 387:138553. doi: 10.1016/j.electacta.2021.138553

25. Wei SS, Xiao HL, Gu M, Chen ZC, Cao LL. Ultrasensitive label-free electrochemical immunosensor based on core-shell Au@PtNPs functionalized rGO-TEPA/PB nanocomposite for HBsAg detection. *J Electroanal Chem.* (2021) 890:9. doi: 10.1016/j.jelechem.2021.115216

26. Ma JL, Yin BC, Wu X, Ye BC. Copper-mediated dna-scaffolded silver nanocluster switch for detection of pyrophosphate and alkaline phosphatase. *Anal Chem.* (2016) 88:9219–25. doi: 10.1021/acs.analchem.6b02465

27. Jin X, Chen L, Zhang YT, Wang XL, Zhou ND, A. lateral flow strip for on-site detection of tobramycin based on dual-functional platinum-decorated gold nanoparticles. *Analyst.* (2021) 146:3608–16. doi: 10.1039/D1AN00403D

28. Chen G, Jin M, Ma J, Yan M, Cui X, Wang Y, et al. Competitive bio-barcode immunoassay for highly sensitive detection of parathion based on bimetallic nanozyme catalysis. *J Agric Food Chem.* (2021) 68:660–8. doi: 10.1021/acs.jafc.9b06125

29. Sajwan RK, Lakshmi G, Solanki PR. Fluorescence tuning behavior of carbon quantum dots with gold nanoparticles *via* novel intercalation effect of aldicarb. *Food Chem.* (2021) 340:9. doi: 10.1016/j.foodchem.2020.127835

30. Wu X, Song Y, Yan X, Zhu C, Ma Y, Du D, et al. Carbon quantum dots as fluorescence resonance energy transfer sensors for organophosphate pesticides determination. *Biosens Bioelectron.* (2017) 94:292–7. doi: 10.1016/j.bios.2017.03.010

31. Eissa S, Zourob M. Selection and characterization of DNA aptamers for electrochemical biosensing of carbendazim. *Anal Chem.* (2017) 89:3138–45. doi: 10.1021/acs.analchem.6b04914

32. Anastassiades M, Lehotay SJ, Stajnbaher D, Schenck FJ. Fast and easy multiresidue method employing acetonitrile extraction/partitioning and "dispersive solid-phase extraction" for the determination of pesticide residues in produce. *J AOAC Int.* (2003) 86:412–31. doi: 10.1093/jaoac/86.2.412

33. Ouyang Q, Wang L, Ahmad W, Rong Y, Li H, Hu Y, et al. A highly sensitive detection of carbendazim pesticide in food based on the upconversion-MnO_2 luminescent resonance energy transfer biosensor. *Food Chem.* (2021) 349:129157. doi: 10.1016/j.foodchem.2021.129157

34. Zhang XL, Wu D, Zhou XX Yu YX, Liu JC, Hu N, et al. Recent progress in the construction of nanozyme-based biosensors and their applications to food safety assay. *TrAC, Trends Anal Chem.* (2019) 121:22. doi: 10.1016/j.trac.2019.115668

35. Wang S, Su L, Wang L, Zhang D, Shen G, Ma Y. Colorimetric determination of carbendazim based on the specific recognition of aptamer and the poly-diallyldimethylammonium chloride aggregation of gold nanoparticles. *Spectrochim Acta, Part A.* (2020) 228:117809. doi: 10.1016/j.saa.2019.117809

36. Zhou Y, Li Y, Han P, Dang Y, Zhu M, Li Q, et al. A novel low-dimensional heteroatom doped Nd_2O_3 nanostructure for enhanced electrochemical sensing of carbendazim. *New J Chem.* (2019) 43:14009–19. doi: 10.1039/C9NJ02778E

37. Zhu X, Liu P, Ge Y, Wu R, Xue T, Sheng Y, et al. MoS_2/MWCNTs porous nanohybrid network with oxidase-like characteristic as electrochemical nanozyme sensor coupled with machine learning for intelligent analysis of carbendazim. *J Electroanal Chem.* (2020) 862:113940. doi: 10.1016/j.jelechem.2020.113940

38. Su L, Wang S, Wang L, Yan Z, Yi H, Zhang D, et al. Fluorescent aptasensor for carbendazim detection in aqueous samples based on gold nanoparticles quenching Rhodamine B. *Spectrochim Acta, Part A.* (2020) 225:117511. doi: 10.1016/j.saa.2019.117511